Movement of oxygen vacancies in oxide film during annealing observed by an optical reflectivity difference technique

Xu Wang, Kuijuan Jin, and Hubin Lu
Beijing National Laboratory for Condensed Matter Physics, Institute of Physics, Chinese Academy of Sciences, Beijing 100080, People's Republic of China

Yiyan Fei
Department of Physics, University of California at Davis, Davis, California 95616, USA

Xiangdong Zhu
Beijing National Laboratory for Condensed Matter Physics, Institute of Physics, Chinese Academy of Sciences, Beijing 100080, People's Republic of China and Department of Physics, University of California at Davis, Davis, California 95616, USA

Guozhen Yang[a)]
Beijing National Laboratory for Condensed Matter Physics, Institute of Physics, Chinese Academy of Sciences, Beijing 100080, People's Republic of China

The monolayer growth of Nb-doped $SrTiO_3$ on $SrTiO_3$ (100) substrate is prepared by a pulsed laser deposition method. The growth and annealing of the film in vacuum and in oxygen ambient are monitored in real time by an oblique-incidence optical reflectivity difference (OIRD) technique and reflection high-energy electron diffraction technique. The films annealed in different ambient result in different optical annealing signals. From the comparison of experimental OIRD signals with the simulation of OIRD signals, we prove that the optical technique can easily tell whether the oxygen vacancies are moving into or moving out of the film during the annealing. The optical signals are found to be composed of contributions from step edges and terraces. © *2007 American Institute of Physics*. [DOI: 10.1063/1.2776375]

I. INTRODUCTION

Perovskite-type oxides have been studied extensively[1–3] in the past because of the importance in fields of basic research and thin-film applications in superconductivity, ferroelectricity, dielectricity, and so on. These properties of oxide films are mostly subject to oxygen content.[4,5] Photoemission studies by many groups have shown that oxygen deficiency in a perovskite crystal is mostly in the form of oxygen vacancies,[6,7] and the rate of diffusion for oxygen vacancies between 630 °C and 800 °C has been reported to be 2–3 orders of magnitude larger than that for oxygen atoms,[8] thus the diffusion of oxygen vacancies during growth and annealing have attracted considerable interest.

Real time monitoring of the growing film is an essential part in the study of oxygen vacancies diffusion. Some techniques have been used to simultaneously monitor the surface, such as low-energy electron microscopy (LEEM), and ellipsometry. Using LEEM, McCarty *et al.* have found that steps on the TiO_2 (110) surface move when the temperature is changed. This is because some material is being added to or subtracted from the surface, caused by the fact that the concentration of bulk oxygen vacancies changes with the temperature.[9] Ellipsometry is often used to measure the changes in both magnitude and phase of complex optical reflectivity (i.e., the Fresnel reflection coefficient) in response to the variation in the roughness and the dielectric properties of solid surfaces. Michaelis *et al.* have studied the oxygen diffusion in $YBa_2Cu_3O_{7-\delta}$ (YBCO) thin films by spectroscopic ellipsometry.[10] Kawasaki *et al.* have observed that the oxygen content of YBCO thin film changes during cooling by a light reflectance variation.[11]

The latter two upper studies point out that optical techniques are appropriate for observation of diffusion of oxygen vacancies. In this article, we report our results of perovskite film growth simultaneously monitored with reflected high energy electron diffraction (RHEED) and an oblique-incidence optical reflectivity difference (OIRD) technique.[12] We found that the annealing in vacuum of the film results in a negative slope of the OIRD annealing signal, while the annealing in oxygen ambient results in a positive slope of the OIRD annealing signal. We further prove from simulation of OIRD signals that a negative slope of annealing signal indicates that the oxygen vacancies are moving into the film.

As for OIRD technique, the experimental setup and procedures have been described previously.[13] Briefly let r_{p0} and r_{s0} denote the respective reflectivity from the bare substrate for *p*- and *s*-polarized light at the wavelength of a He-Ne probe laser $\lambda = 632.8$ nm, and r_p and r_s be the respective reflectivity during the growth. Fractional changes in reflectivity are defined as $\Delta_p = |(r_p - r_{p0})/r_{p0}|$ and $\Delta_s = |(r_s - r_{s0})/r_{s0}|$. We measure the difference defined as $\mathrm{Re}\{\Delta_p - \Delta_s\}$ in the OIRD technique. Zhu *et al.* have claimed that this technique is a particular form of optical ellipsometry.[14]
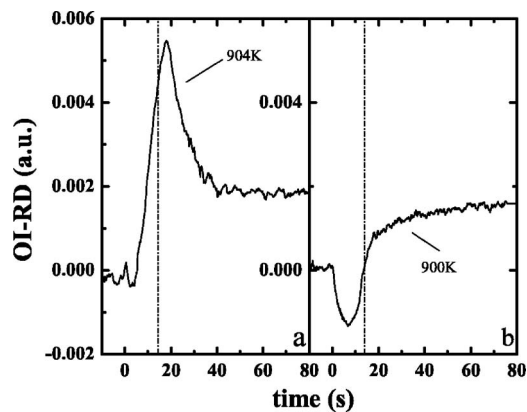

[a)]Electronic mail: yanggz@aphy.iphy.ac.cn

FIG. 1. OIRD signals for monolayer growth of Nb:SrTiO$_3$ on SrTiO$_3$ (001) at high temperature in oxygen free ambient (a) and oxygen ambient (b). The dash-dot line remarks the completion of the deposition of one monolayer.

FIG. 2. OIRD signals (black curve) during the growth of an intermittent deposition of one Nb:SrTiO$_3$ monolayer on SrTiO$_3$ (001) in vacuum at temperature of 1003 K. The gray curve shows a simulated result.

II. EXPERIMENTAL AND SIMULATED RESULTS

The growths were performed in a chamber with a base pressure of 1×10^{-5} Pa (7.5×10^{-8} Torr). The chamber was equipped with a standard RHEED apparatus and an OIRD measurement system. The SrTiO$_3$ substrate of $10 \times 5 \times 0.5$ mm^3 was attached to a stainless heater block in the chamber. These substrates had been treated to have regular step edges on top.[15] The temperature of the substrate was monitored by an optical pyrometer during the deposition. A sintered ceramics of stoichiometric Nb:SrTiO$_3$ (10 mol %) was used as the target. A 308-nm XeCl excimer laser was used for ablation. The films usually were grown in continuous or intermittent modes with Laser-MBE (Ref. 16) technique. In a continuous mode, the growth was kept going all the while and there was no annealing applied. When the temperature was appropriate for the growth, the RHEED intensity would oscillate for periodically changing surface morphology. The appropriate temperature and the number (N) of laser pulses for growing monolayer material in continuous mode also fit for the intermittent mode. In the intermittent mode, we first deposited one monolayer of materials ($0 < t < t_1$, t_1 is when the growth is finished), then we interrupted the deposition and made the film annealing for a period of time ($t_1 < t < t_2$, $t_2 - t_1$ is the annealing time). After that, we deposited the next monolayer material. This process was repeated in the intermittent growth.

With temperatures above 900 K, even in oxygen-free ambient, the specular RHEED intensity recovers to the predeposition level essentially right after a monolayer equivalent of Nb:SrTiO$_3$ is deposited.[17] Figures 1(a) and 1(b) show the OIRD signals of intermittent monolayer growth in oxygen free ambient and oxygen ambient with nearly the same temperature 900 K. The two signals show very clearly that the annealing in different ambient after the monolayer growth leads to different slope of OIRD signals. Another example (black curve) is shown in Fig. 2. We performed the intermittent growth in oxygen free ambient at 1003 K. This optical signal is similar to the one in Fig. 1(a), except the small tip at the beginning of the growth in Fig. 1(a) becomes an evident downward peak in Fig. 2. From these two figures and other experimental data,[17,18] we get some characters
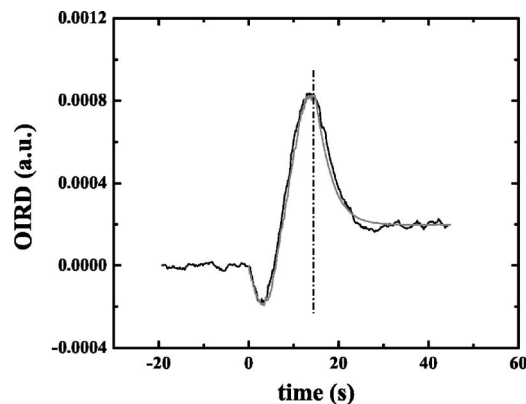
from the optical signals. First, *the optical signals all have a downward tip near the beginning of the growth* no matter in oxygen ambient or oxygen free ambient. These downward tips appear at different times and they often appear before the surface is roughest. Second, *a positive slope of annealing signal corresponds to oxygen ambient*, *while a negative slope of annealing signal corresponds to oxygen-free ambient*. To determine where the tip comes from and whether the different slopes of annealing signals indicate different diffusions of oxygen vacancies, we need to simulate the optical signal and find where the optical signal comes from.

The simulation of optical signals includes two parts. First, we simulated the growth with the Monte Carlo method to get the information of the surface. Then we calculated optical reflectance difference signal from the surface.

Dielectric functions of the films are useful for analysis of their oxygen content.[11] By simulating the optical signals from a growing film, we may get information about these dielectric functions in film. For convenience, Zettler *et al.* reduced the three media system (ambient, film, substrate) into only two media (ambient, effective substrate) in their model.[19] They simply found the dielectric function of the effective substrate oscillates in the growth. To model the system more exactly, four media system (ambient, surface, film, substrate) is used in our work. As shown by Kalff *et al.*,[20] Vrijmoeth *et al.*,[21] and others in scanning tunneling microscopy studies of epitaxy and ion erosion of crystalline metals, a majority of surface atoms on a growth or erosion surface are on terraces and a minority of them are nearby step edges. In this case, to describe a more real system, we further divide the surface into two parts: terrace atoms and step edge atoms, and set ε_{terr} and ε_{step} as the dielectric functions of them. Since the imaginary part of the dielectric function is associated with the oxygen vacancy concentration,[22] the study on these dielectric functions is expected to reveal how the oxygen vacancies move.

Monte Carlo simulation has shown that surface step density can successfully reproduce the RHEED specula intensity qualitatively[23,24] and quantitatively,[25] which means the Monte Carlo method is an effective way to simulate the surface morphology. By simulating the deposition process with the Monte Carlo method[26,27] and modeling the surface struc-

ture with a mean-field model,[28] how the numbers of step edge atoms and terrace atoms are changing with time during the growth could be achieved. In the Monte Carlo simulation with periodical boundary conditions (no boundary-dependent effects[29] are expected), the unit cell is treated as a cubic growth unit, whose mobility and the nearest-neighbor bonding of units were isotropic (the solid-on-solid model[30]). The growth kinetics is described as two processes: the deposition of units onto the substrate at random sites and subsequent migration of surface units driven by binding energy until incorporation into or emission form the growth front. With the surface morphology changing with time, we collect a statistic of numbers of step edge atoms and terrace atoms on surface to get the coverage of them and calculate the reflectivity for *s*- and *p*-polarized light as the sum of contribution from all units[28]

$$r_{s(p)} = \sum_{j=0} r_{s(p)}^{(t)}(d_j)\, \theta_{j,\text{terr}} \exp[-i4\pi(d_j - \langle d \rangle)\cos\,\phi_{inc}/\lambda]$$
$$+ \sum_{j=0} r_{s(p)}^{(\text{step})}(d_j)\, \theta_{j,\text{step}} \exp[-i4\pi(d_j - \langle d \rangle)\cos\,\phi_{inc}/\lambda],$$

$$(1)$$

where $\theta_{i,\text{errt}}$ is the coverage of the *j*th "coalesced" terrace atoms at a distance $d_j = jd_0$ away from the top surface, $\theta_{i,\text{step}}$ is the corresponding coverage of step edge atoms, d_0 is the thickness of one monolayer in the direction normal to the substrate, and d_j is the height of each unit, $\langle d \rangle$ is the average thickness of film, ϕ_{inc} denotes the incident angle, and the total coverage of step edge atoms is $\theta_{\text{step}} = \Sigma_{i=0}\theta_{i,\text{step}}$. $r_{s(p)}^{(*)}(d_j)$ is the reflectivity of one unit for *s*(*p*)-polarized light from a four media system that consists of vacuum, a monolayer of surface atoms ($r_{s(p)}^{(\text{step})}(d_j)$ for step edge atoms; $r_{s(p)}^{(t)}(d_j)$ for terrace atoms), a layer of bulk-phase film, and the substrate. At last, we calculate $\text{Re}\{\Delta_p - \Delta_s\}$ as OIRD signals. By simulating OIRD experimental signals, we get the dielectric functions in film system during the growth.

We have made some simplifications and assumptions in the simulation of intermittent OIRD signals. During the growth period, the materials were kept sputtering on the sur-
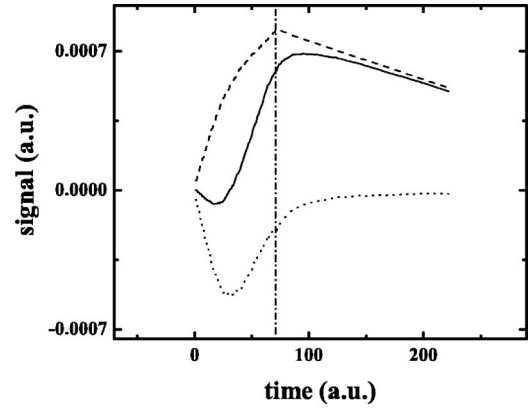

FIG. 3. The solid line shows a simulated optical signal in intermittent mode. The dash line and the dot line show contributions from terrace atoms and step edge atoms.

face. It would be difficult to consider the oxidization or deoxidization for all the just sputtered materials, which requests dielectric functions changing with time for materials with different life times. So we ignore the oxidization or deoxidization during growth and give the sputtering materials an average constant dielectric function. While the considerable change of the surface morphology during the growth period should be taken into account. In an intermittent growth, at the time when the monolayer growth is completed, the quantity of step edge atoms is very small compared with the quantity of the terrace atoms, that we ignore the variations of the dielectric functions of step edge atoms during post-deposition annealing. So, if the oxidization or deoxidization process takes place in post-deposition annealing, only the dielectric function of the terrace atoms would be changing with time. Besides, due to the periodicity of intermittent growth signals, it is further supposed in simulation that during the post-deposition annealing $\varepsilon_{\text{terr}}$ simply changes from ε_{t0} to the dielectric function of the bulk film linearly with time. ε_{t0} was the constant dielectric function for terrace atoms in growth period. Consequently the dielectric functions for step edge atoms and terrace atoms during growth period and annealing period are below

$$\begin{cases} \varepsilon_{\text{step}}(t) = \varepsilon_{s0} & 0 < t < t_2 \\ \varepsilon_{\text{terr}}(t) = \varepsilon_{t0} & 0 < t < t_1;\ \varepsilon_{\text{terr}}(t) = \varepsilon_{t0} + \text{const} \times t, \quad t_1 < t < t_2. \end{cases} \qquad (2)$$

It should be noted that in this article we focused on only the imaginary part of the dielectric functions. Information from the real part of the dielectric functions was ignored.

From Eq. (1), we can see that the optical signal has contributions from terrace atoms and step atoms: $\text{Signal}_{\text{total}} = \text{Signal}_{\text{terr}} + \text{Signal}_{\text{step}}$. It is difficult to get analytic expression for each component, but we can try to separate them in the numerical calculation. A simulated result with annealing in vacuum is shown in Fig. 3. The solid line shows $\text{Signal}_{\text{total}}$,

the dash line shows $\text{Signal}_{\text{terr}}$, and the dotted line shows $\text{Signal}_{\text{step}}$. In Fig. 4, the step density in the simulated monolayer growth and the coverage of the terrace atoms formed just during the simulated monolayer growth are also shown. It is clear that the $\text{Signal}_{\text{step}}$ looks similar to specular RHEED intensity that is related with step density. The contrast of the $\text{Signal}_{\text{step}}$ and the step density shows that the contribution of step edge atoms is roughly inverse proportional to step density. As to $\text{Signal}_{\text{terr}}$, it increases in the growth period and
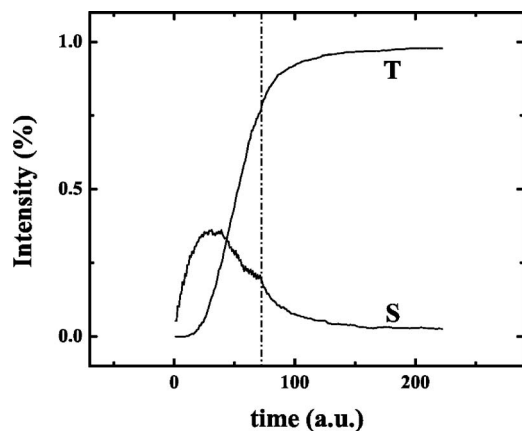
FIG. 4. The step density (S) in the simulated monolayer growth and the coverage (T) of the terrace atoms formed just during the simulated monolayer growth.

decreases in the annealing period. It is understandable that the contribution of terrace atoms first increases because of the increasing atoms of the new-formed terrace in growth period. However, after the growth is finished and the coverage of new-formed terrace atoms changes very little in the annealing period, why does the Signal$_{\text{terr}}$ decrease? To make it clear, we have adjusted the parameters in the procedure for many times, and we found that the decrease of Signal$_{\text{terr}}$ is caused by the increase of the imaginary part of the dielectric function of terrace atoms (Im($\varepsilon_{\text{terr}}$)) on surface in annealing period. Actually, if Im($\varepsilon_{\text{terr}}$) decreases in annealing period, the Signal$_{\text{terr}}$ will increase in annealing.

In short, the optical signal comes from both terrace atoms and step edge atoms. Since the dielectric functions for step edge atoms and terrace atoms are different, the increase in amount of step edge atoms and the terrace atoms both contribute to OIRD signals but with different weight coefficients. By doing more simulations and based on Eq. (1), we conclude a simple analytical expression for the OIRD signal: Signal$_{\text{total}} \approx A(\text{Im}(\varepsilon_{\text{terr}})) \cdot \theta_{\text{terr}} - B(\text{Im}(\varepsilon_{\text{step}})) \cdot \theta_{\text{step}}$. Here, θ_{terr} and θ_{step} are total coverage for terrace atoms and step edge atoms, $A(x)$ and $B(x)$ are still undetermined functions. But at least we know $A(x)$ is a decreasing function with x from simulated results. So the change of Im($\varepsilon_{\text{terr}}$) results in reverse change of the optical signal. Besides, in the simulation we made Im($\varepsilon_{\text{terr}}$) change linearly with time in the annealing which led to an linear annealing signal shown in Fig. 3. But an experimental annealing signal in Fig. 2 changes with time more like an exponential function. This disagreement indicates that Im($\varepsilon_{\text{terr}}$) would probably change with time as an exponential function in annealing. With this conclusion, the simulated result (gray curve in Fig. 2) reproduced the main characteristics of experimental signal better, which indicates the simulation procedure is now appropriate.

In different growth conditions, the dielectric functions for each material might be different. So, $A(\text{Im}(\varepsilon_{\text{terr}}))$ would be different for different $\varepsilon_{\text{terr}}$ and $B(\text{Im}(\varepsilon_{\text{step}}))$ would be different for different $\varepsilon_{\text{step}}$. That explains why the tips of OIRD signals appear at different times in different growth conditions. Since only the step edge atoms contribute to RHEED signals or step density, this also explains why the tip of

OIRD signal does not appear when the surface is roughest. As to the annealing signal, since we ignore contribution from step edge atoms in an annealing period, the decrease of the optical signal only indicates the decrease of $A(\text{Im}(\varepsilon_{\text{terr}}))$ or the increase of Im($\varepsilon_{\text{terr}}$). The increase of Im($\varepsilon_{\text{terr}}$) means that the oxygen vacancy concentration of the surface is increasing. So annealing in oxygen-free ambient, the oxygen vacancies are moving into the film. Similarly, the optical signal increases in annealing in oxygen ambient comes to a conclusion that the oxygen vacancies are moving out of the film in annealing in oxygen ambient. Form the comparison of OIRD signals in different growing conditions above 900 K, it is clear that a higher temperature or a higher oxygen pressure (or the combination of them both) makes the tip of OIRD signals more evident, which requests a bigger $B(\text{Im}(\varepsilon_{\text{step}}))$ or a smaller $A(\text{Im}(\varepsilon_{\text{terr}}))$. Since these possibilities can both be proved by simulation, it is still uncertain what the actual process is.

III. CONCLUSIONS

In summary, by analyzing the OIRD signals during post-deposition annealing and simulating the OIRD signals, we find the OIRD technique is quite appropriate to real-time monitoring of oxide film growth. The OIRD signal includes two components: contributions from step edges and terraces, and can be described as Signal$_{\text{total}} \approx A(\text{Im}(\varepsilon_{\text{terr}})) \cdot \theta_{\text{terr}} - B(\text{Im}(\varepsilon_{\text{step}})) \cdot \theta_{\text{step}}$. The terrace atoms are the main part of the surface during annealing. So the change of Im($\varepsilon_{\text{terr}}$) in annealing informs how the oxygen vacancies are moving. We prove that basically oxygen vacancies are moving out of the film during annealing in oxygen ambient while moving into the film during annealing in vacuum. Detailed studies on films with different growth conditions are expected in a future work

[1] J. Junquera and P. Ghosez, Nature **422**, 506 (2003).
[2] P. Pertosa and F. M. Michel-Calendini, Phys. Rev. B **17**, 2011 (1978).
[3] A. Ohtomo and H. Y. Hwang, Nature **427**, 423 (2003).
[4] H. L. Ju, J. Gopalakrishnan, J. L. Peng, Q. Li, G. C. Xiong, T. Venkatesan, and R. L. Greene, Phys. Rev. B **51**, 6143 (1995).
[5] J. P. Sydow, R. A. Ruhrman, and B. H. Moeckly, Appl. Phys. Lett. **72**, 3512 (1998).
[6] R. Moos, W. Menesklou, and K. H. Hardtl, Appl. Phys. A: Mater. Sci. Process. **61**, 389 (1995).
[7] A. Hirata, A. Ando, K. Saiki, and A. Koma, Surf. Sci. **310**, 89 (1994).
[8] P. Pasierb, S. Komornicki, and M. Rekas, J. Phys. Chem. Solids **60**, 1835 (1999).
[9] K. F. McCarty and N. C. Bartelt, Phys. Rev. Lett. **90**, 046104 (2003).
[10] A. Michaelis, E. A. Irene, O. Auciello, and A. R. Krauss, J. Appl. Phys. **83**, 7736 (1998).
[11] N. Kanda, M. Kawasaki, K. Nakano, and T. Shirashi, Jpn. J. Appl. Phys., Part 1 **36**, 2103 (1997).
[12] X. D. Zhu, H. B. Lu, G. Z. Yang, Z. Y. Li, B. Y. Gu, and D. Z. Zhang, Phys. Rev. B **57**, 2514 (1998).
[13] X. D. Xiao, Y. L. Xie, and Y. R. Shen, Surf. Sci. **271**, 295 (1992).
[14] X. D. Zhu, Opt. Commun. **259**, 751 (2006).
[15] X. Wang, Y. Y. Fei, H. B. Lu, K. J. Jin, X. D. Zhu, Z. H. Chen, Y. L. Zhou, and G. Z. Yang, Sci. China, Ser. G **48**, 459 (2005).

[16] G. Z. Yang, H. B. Lu, H. S. Wang, D. F. Cui, H. Q. Yang, H. Wang, Y. L. Zhou, and Z. H. Chen, Chin. Phys. Lett. **14**, 478 (1997).

[17] F. Chen, T. Zhao, Y. Y. Fei, H. B. Lu, Z. H. Chen, G. Z. Yang, and X. D. Zhu, Appl. Phys. Lett. **80**, 2889 (2002).

[18] X. D. Zhu, Y. Y. Fei, H. B. Lu, and G. Z. Yang, Appl. Phys. Lett. **87**, 051903 (2005).

[19] J. T. Zettler, T. Wethkamp, M. Zorn, M. Pristovsek, C. Meyne, K. Ploska, and W. Richter, Appl. Phys. Lett. **67**, 3783 (1995).

[20] M. Kalff, G. Comsa, and T. Michely, Surf. Sci. **486**, 103 (2001).

[21] J. Vrijmoeth, H. A. Vandervegt, J. A. Meyer, E. Vlieg, and R. J. Behm, Phys. Rev. Lett. **72**, 3843 (1994).

[22] X. D. Zhu, W. D. Si, X. X. Xi, Q. Li, Q. D. Jiang, and M. G. Medici, Appl.

[23] V. S. Achutharaman, N. Chandrasekhar, T. Valls Orioll, and A. M. Goldman, Phys. Rev. B **50**, 8122 (1994).

[24] T. Shitara, D. D. Vvedensky, M. R. Wilby, J. Zhang, J. H. Neave, and B. A. Joyce, Phys. Rev. B **46**, 6815 (1992).

[25] P. Šmilauer and D. D. Vvedensky, Phys. Rev. B **48**, 17603 (1993).

[26] F. Chen, H. B. Lu, T. Zhao, K. J. Jin, Z. H. Chen, and G. Z. Yang, Phys. Rev. B **61**, 10404 (2000).

[27] K. J. Jin, S. H. Pan, and G. Z. Yang, Surf. Sci. **380**, 522 (1997).

[28] X. D. Zhu, Phys. Rev. B **69**, 115407 (2004).

[29] S. Clarke and D. D. Vvedensky, Phys. Rev. Lett. **58**, 2235 (1987).

[30] J. D. Weeks and G. H. Gilmer, Adv. Chem. Phys. **40**, 157 (1979).

Phys. Lett. **74**, 3540 (1999).